-

Supporting Information

Photo-activated Time-dependent Color-changeable Ultralong Organic Room Temperature Phosphorescence by Co-doping Strategy

Huiwen Jin,[a] Xue Zhang,[a] Zhimin Ma,[b] Chen Qian,[a] Xiaohua Fu,[a] Zewei Li,[b] Mingxing Chen,[b] Yan Guan[b] and Zhiyong Ma[a]*

[a] Prof. Z.Y. Ma, Miss. H.W. Jin, Miss. X. Zhang, Mr. C. Qian, Mr. X.H. Fu
Beijing Advanced Innovation Center for Soft Matter Science and Engineering, State Key Laboratory of Organic-Inorganic Composites, College of Chemical Engineering, Beijing University of Chemical Technology, Beijing 100029, China. E-mail: mazhy@mail.buct.edu.cn.

[b] Dr. Z.M. Ma, Dr. Y.Guan. Dr. M.X. Chen, Mr. Z.W. Li
Beijing National Laboratory for Molecular Sciences, Key Laboratory of Polymer Chemistry and Physics of the Ministry of Education, College of Chemistry and Molecular Engineering, Peking University, Beijing 100871, China.

Supporting information for this article is given via a link at the end of the document.

Table of Contents

1. Materials and General Methods

All the solvents and reactants were purchased from commercialized companies and used as received without further purification except for specifying otherwise.

^{1}H NMR was recorded on the 400 MHz (Bruker ARX400) and ^{13}C NMR spectra were recorded on the Bruker 101 MHz spectrometer at room temperature with $CDCl_3$, DMSO-d_6 and *d*-DMF as the solvents and tetramethylsilane (TMS) as the internal standard. ESI high resolution mass-spectra (HRMS) were acquired on a Waters Xevo G2 Qt of mass spectrometer. High Performance Liquid Chromatography (HPLC) was also acquired on Xevo G2 Qtof. The elution procedure was optimized as 65/35 (v/v) of acetonitrile/water for 15 min at 1.00 mL/min. Transient and delayed photoluminescence spectra were performed on the Hitachi F-4600 or Edinburgh Instruments FLS980 fluorescence spectrophotometer. Luminescence lifetime were acquired on the Edinburgh Instruments FLS980 fluorescence spectrophotometer or Deltaflex Fluorescence Lifetime Instrument (λ_{ex}=365 nm).

TD-DFT calculations were conducted on Gaussian 09 program with a method similar to previous literature.[1] Ground state (S_0) geometries of CN2BCzBr and CNCzBCzBr monomer were directly optimized in vacuum condition. On the basis of this, exciton energies in singlet (S_n) and triplet states (T_n) were estimated through a combination of TDDFT and B3LYP at the 6-311+G(p, d) level. We have to emphasize that the computed singlet and triplet levels in this article refer to emission (excited state optimization). Kohn-Sham frontier orbital analysis was subsequently performed based on the results of theoretical calculation to elucidate the mechanisms of possible singlet-triplet intersystem crossings, in which the channels from S_1 to T_n were believed to share part of the same transition orbital compositions. Herein, energy levels of the possible T_n states were considered to lie within the range of ES_1±0.3 eV.[2] Spin-orbital couplings (SOC) matrix elements were conducted through the Beijing Density Functional (BDF) program based on optimized.

2. Syntheses and characterizations

The synthesis methods of the target molecules (CN2BCzBr and CNCzBCzBr) used in this paper are the same as our previous work.[3,4] To avoid interference from impurities, Cz was also synthesized from aniline and o-bromoiodobenzene through two steps of reactions according to the procedures in our previous work.[4] The detailed syntheses of CN2BCzBr and CNCzBCzBr are shown as follows.

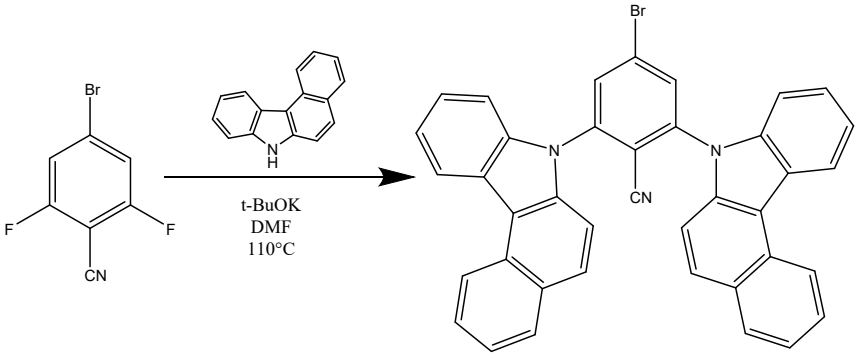

Scheme S1. The synthetic route to CN2BCzBr.

CN2BCzBr: A mixture of 7H-Benzo[c]carbazole (0.2398 g, 2.2 mmol), 4-bromo-2,6-difluorobenzonltrlle (0.2390 g, 1.1 mmol) and t-BuOK (0.3366 g, 3 mmol) were dissolved in DMF (10 mL) in a Schlenk bottle and was stirred under N_2 atmosphere for 24 h at 110 °C. After the reaction was over, the resultant mixture was cooled down to room temperature and the solvent was removed under reduced pressure. The crude product was purified by column chromatography using dichloromethane and petroleum ether (v/v, 1:5) as the eluent to obtain pure product as a white powder. Yield: 45%.

^{1}H NMR (400 MHz, Chloroform-*d*) δ 8.85 (d, J = 8.4 Hz, 2H), 8.67 (d, J = 7.5 Hz, 2H), 8.08 – 7.96 (m, 6H), 7.77 (t, J = 7.6 Hz, 2H), 7.61 – 7.48 (m, 10H).

^{13}C NMR (101 MHz, Chloroform-d) δ 143.22, 139.69, 137.99, 132.82, 130.05, 129.74, 129.38, 128.28, 127.47, 125.30, 124.91, 123.97, 123.54, 122.69, 122.18, 117.01, 112.66, 112.50, 110.74, 110.04.

HR-ESI-MS Calcd. For $C_{39}H_{22}BrN_3$ $[M+H]^+$: 629.1335. Found: 629.1341.

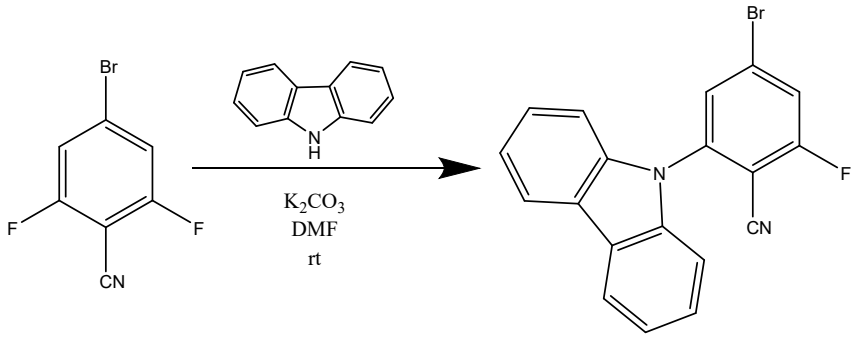

Scheme S2. The synthetic route to CNCzBrF.

CNCzBrF: A mixture of Carbazole (0.8360 g, 5 mmol), 4-bromo-2,6-difluorobenzonltrlle (1.090 g, 5 mmol) and K_2CO_3 (1.0365 g, 7.5 mmol) were dissolved in DMF (10 mL) in a Schlenk bottle and was stirred under N_2 atmosphere for 12 h at room temperature. After the reaction was over, the solvent was removed under reduced pressure. The crude product was purified by column chromatography using dichloromethane and petroleum ether (v/v, 1:10) as the eluent to obtain pure product as a white powder. Yield: 70%.

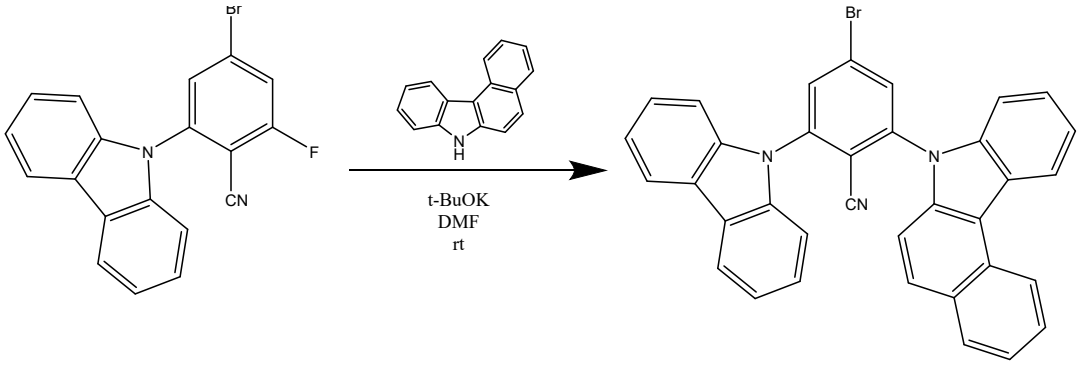

Scheme S3. The synthetic route to CNCzBCzBr.

CNCzBCzBr: A mixture of CNCzBrF (0.2950 g, 0.8 mmol), 7H-Benzo[c]carbazole (0.1738 g, 0.8 mmol) and t-BuOK (0.1347 g, 1.2 mmol) were dissolved in DMF (10 mL) in a Schlenk bottle and was stirred under N_2 atmosphere for 24 h at room temperature. After the reaction was over, the solvent was removed under reduced pressure. The crude product was purified by column chromatography using dichloromethane and petroleum ether (v/v, 1:5) as the eluent to obtain pure product as a white powder. Yield: 63%.

^{1}H NMR (400 MHz, Chloroform-*d*) δ 8.89 – 8.82 (m, 1H), 8.70 – 8.64 (m, 1H), 8.16 (dq, J = 7.6, 1.0 Hz, 2H), 8.05 (d, J = 8.1 Hz, 1H), 8.03 – 7.94 (m, 3H), 7.77 (ddd, J = 8.4, 6.9, 1.3 Hz, 1H), 7.61 – 7.47 (m, 7H), 7.47 – 7.34 (m, 4H), 1.28 (d, J = 13.9 Hz, 1H).

^{13}C NMR (101 MHz, Chloroform-*d*) δ 143.64, 143.21, 140.31, 139.73, 138.04, 132.35, 130.03, 129.75, 129.38, 129.13, 128.26, 127.45, 126.63, 125.27, 124.89, 124.37, 123.94, 123.54, 122.67, 122.13, 121.63, 120.87, 116.97, 112.64, 112.23, 110.78, 110.03, 109.72.

HR-ESI-MS Calcd. For $C_{35}H_{20}BrN_3$ $[M+H]^+$: 579.1179. Found: 579.1181.

3. NMR spectra, HR-MS and HPLC of mentioned molecules.

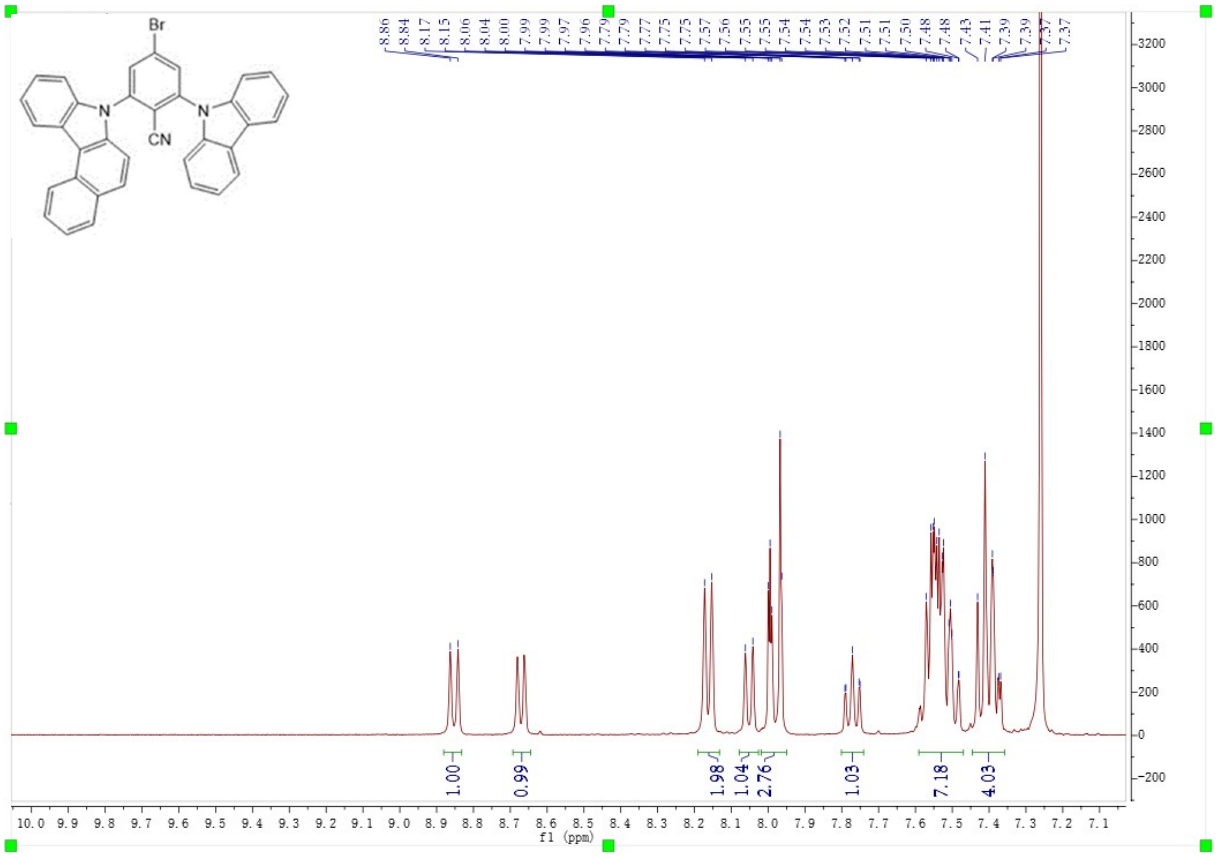

Figure S1. ^{1}H NMR spectrum of CNCzBCzBr in $CDCl_3$.

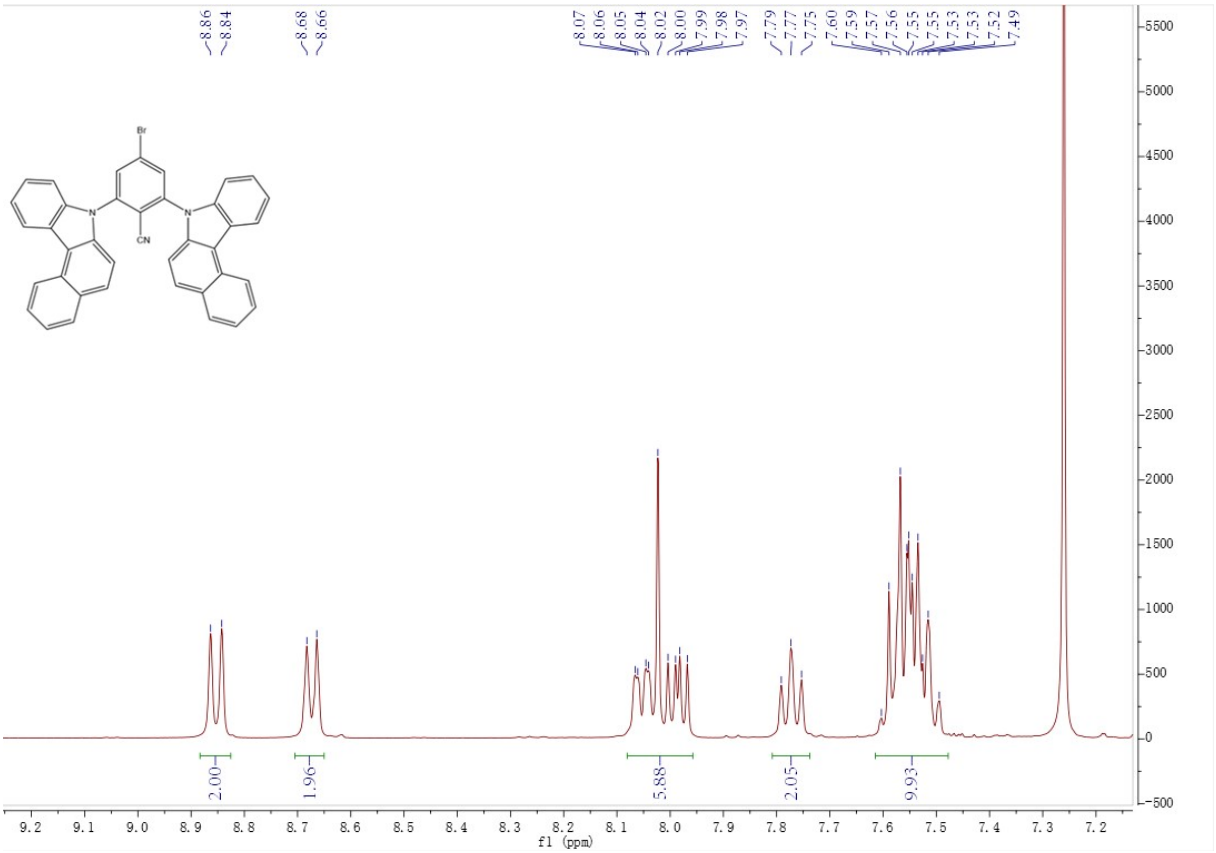

Figure S2. ^{1}H NMR spectrum of CN2BCzBr in $CDCl_3$.

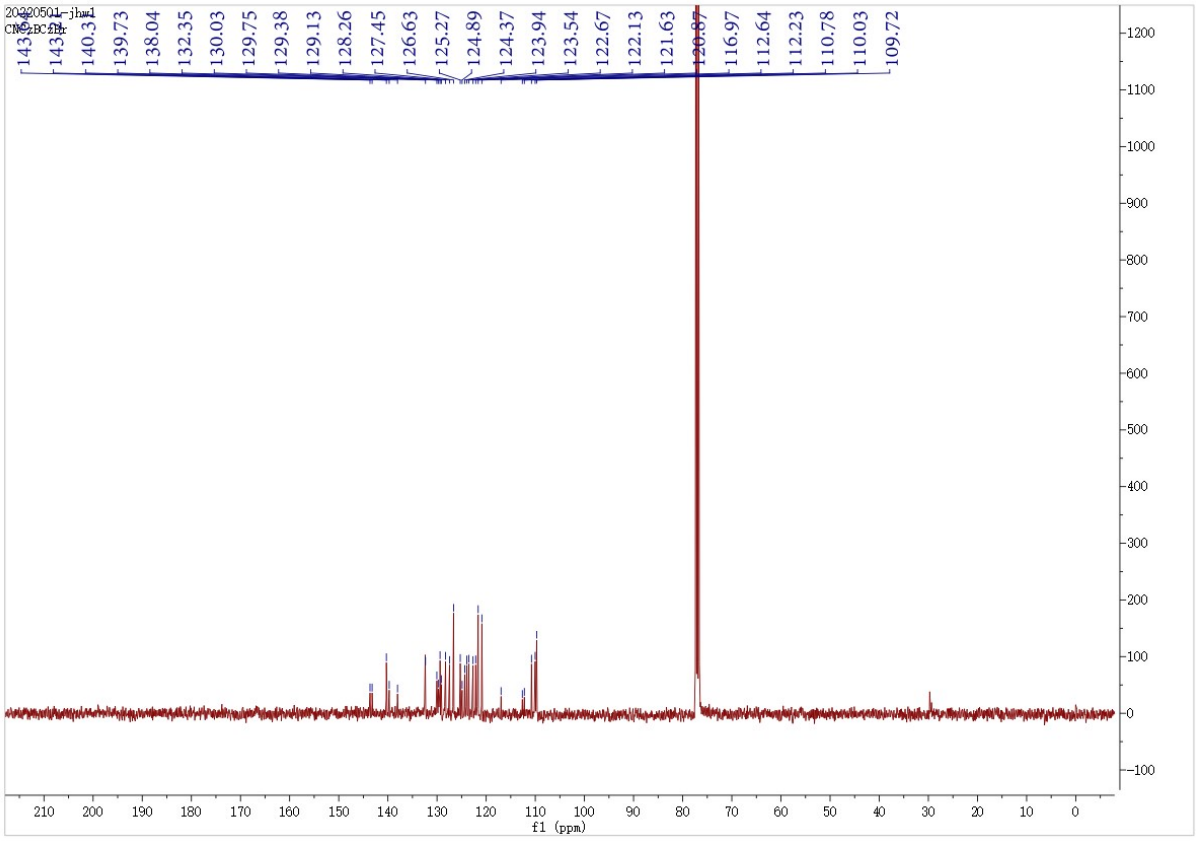

Figure S3. ^{13}C NMR spectrum of CNCzBCzBr in $CDCl_3$.

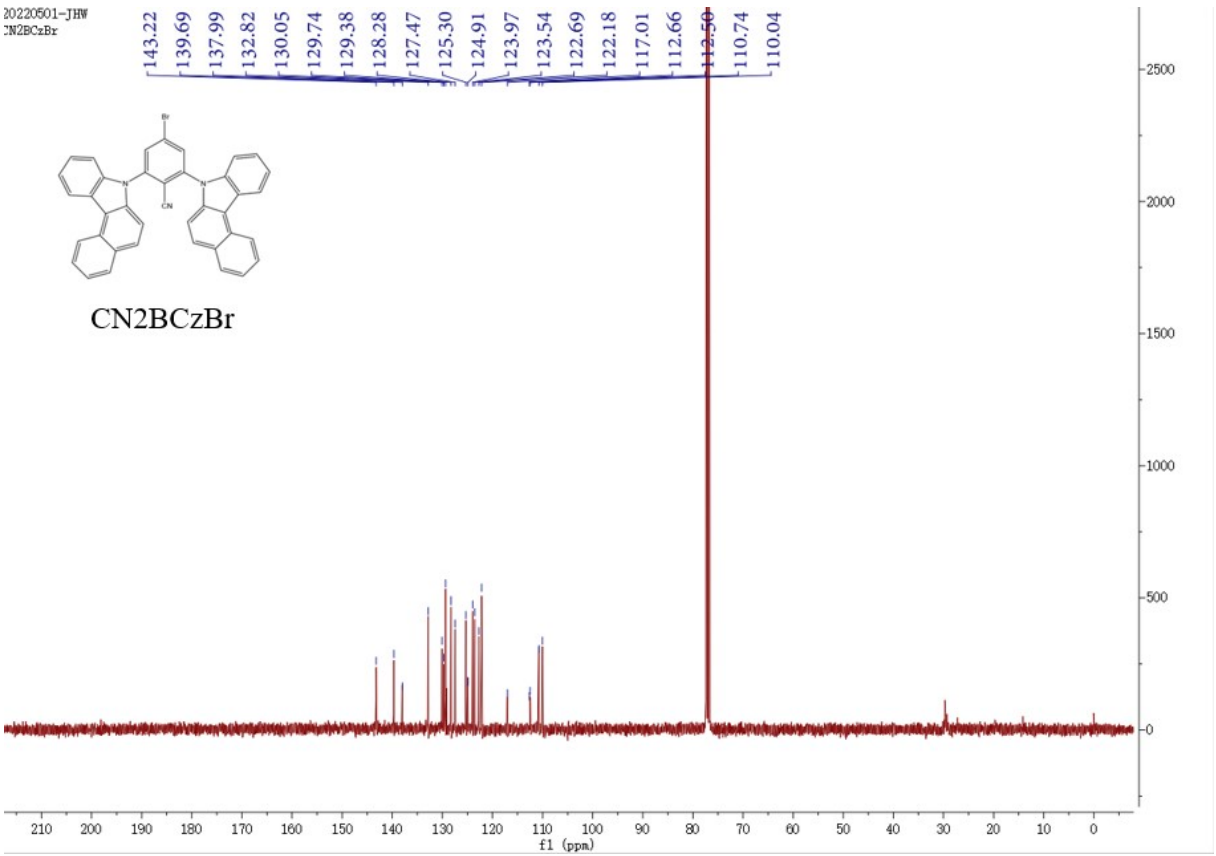

Figure S4. ^{13}C NMR spectrum of CN2BCzBr in $CDCl_3$.

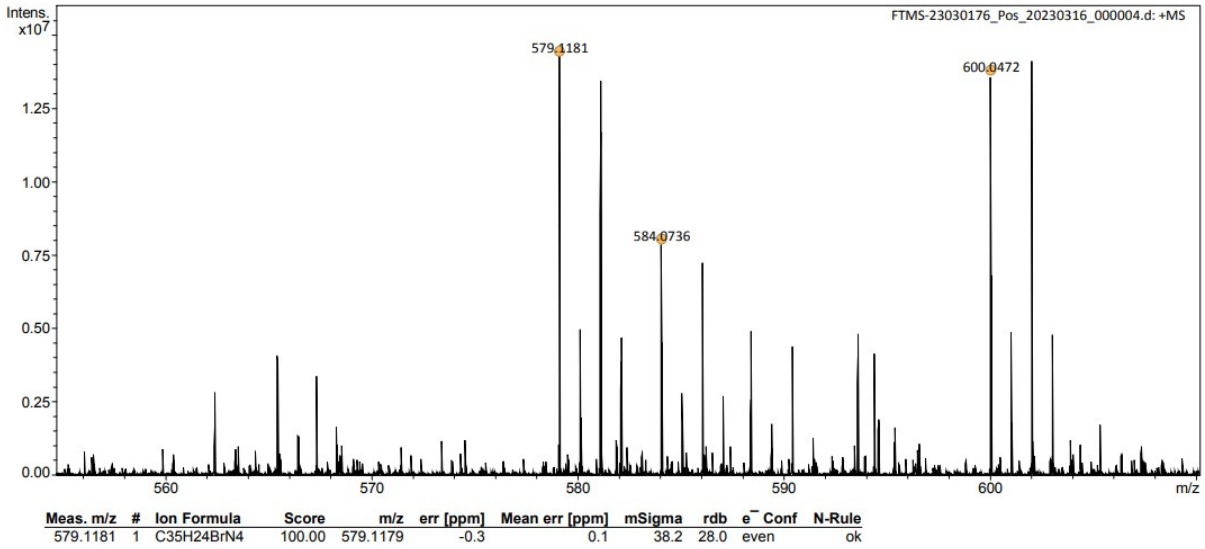

Meas. m/z	#	Ion Formula	Score	m/z	err [ppm]	Mean err [ppm]	mSigma	rdb	e⁻ Conf	N-Rule
579.1181	1	C35H24BrN4	100.00	579.1179	-0.3	0.1	38.2	28.0	even	ok

Figure S5. HR-MS spectrum of CNCzBCzBr.

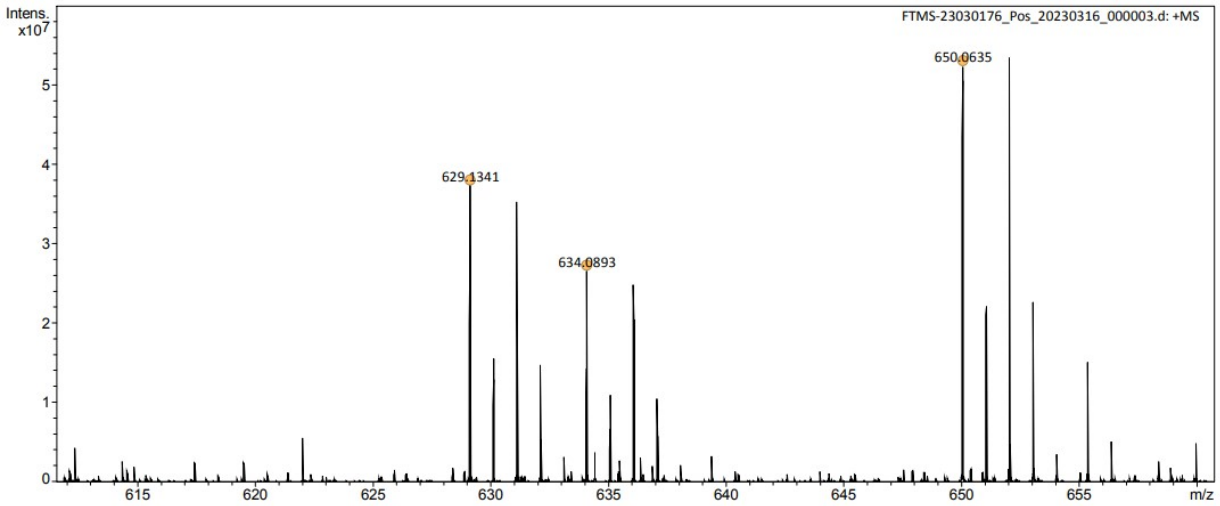

Meas. m/z	#	Ion Formula	Score	m/z	err [ppm]	Mean err [ppm]	mSigma	rdb	e⁻ Conf	N-Rule
629.1341	1	C39H26BrN4	100.00	629.1335	-0.9	-0.6	36.2	31.0	even	ok

Figure S6. HR-MS spectrum of CN2BCzBr.

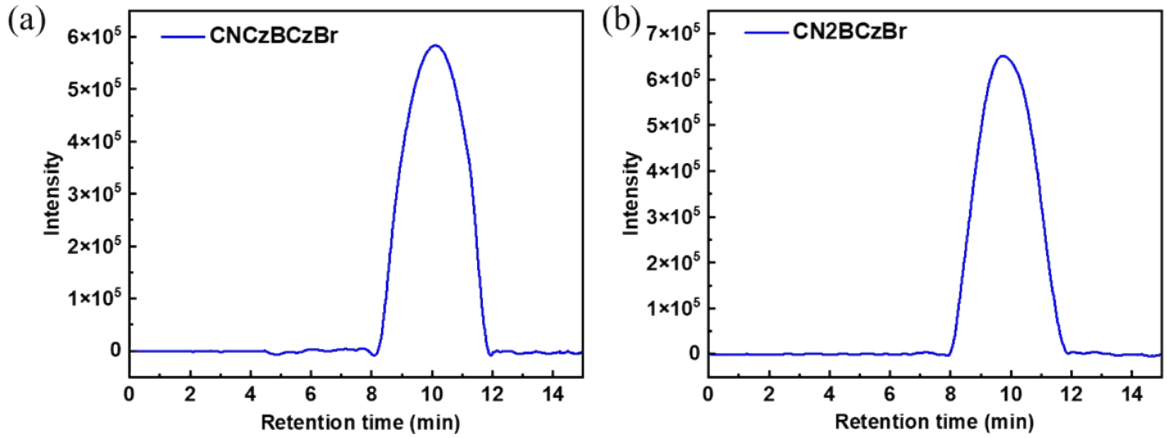

Figure S7. HPLC profiles of CNCzBCzBr and CN2BCzBr.

4. Photophysical properties in the solution

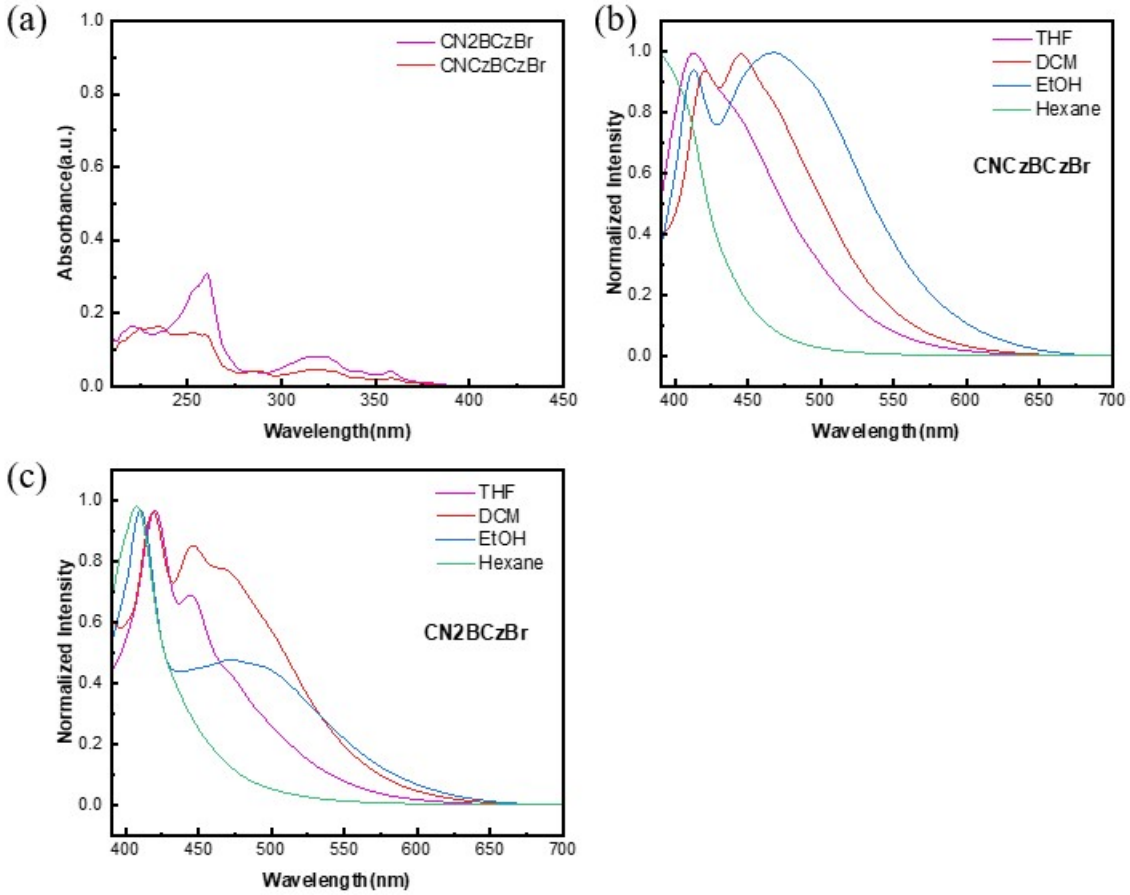

Figure S8. (a) Absorption spectra of BCz derivatives in THF solution; and (b-c) PL spectra of CNCzBCzBr and CN2BCzBr in dilute solution. (20 μM, λ_{ex} = 365 nm)

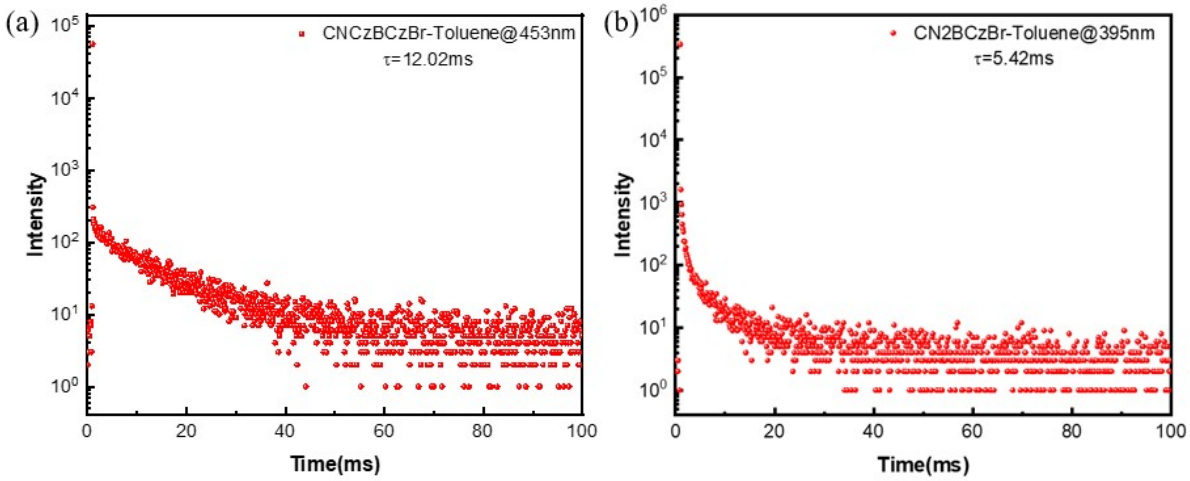

Figure S9. Decay spectra of (a) CNCzBCzBr and (b) CN2BCzBr toluene solution at 77 K.

5. Photophysical properties in the solid state

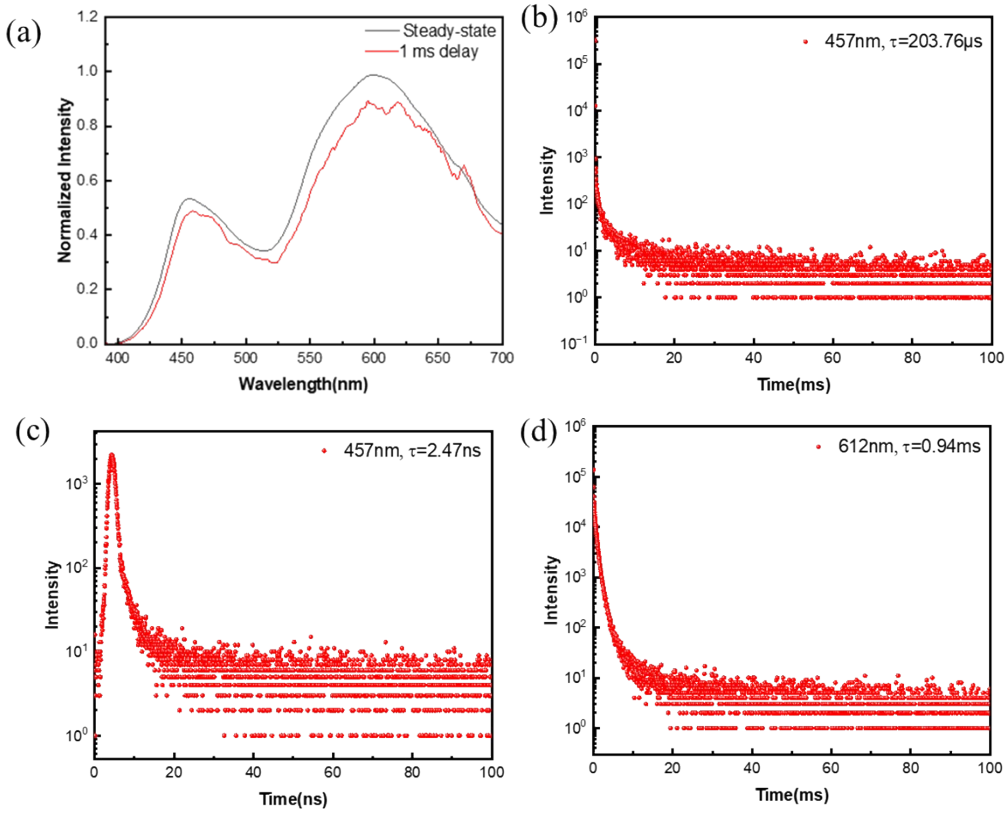

Figure S10. (a) Steady-state and 1 ms-delayed PL spectra of CNCzBCzBr powder; and (b-d) decay spectra at ambient condition. (λ_{ex} = 365 nm)

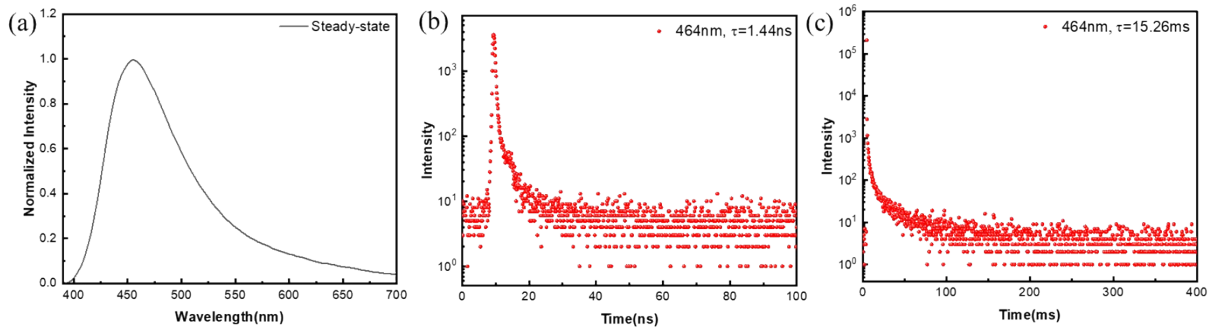

Figure S11. (a) Steady-state spectra of CN2BCzBr powder; and (b-c) decay spectra at ambient condition. (λ_{ex} = 365 nm)

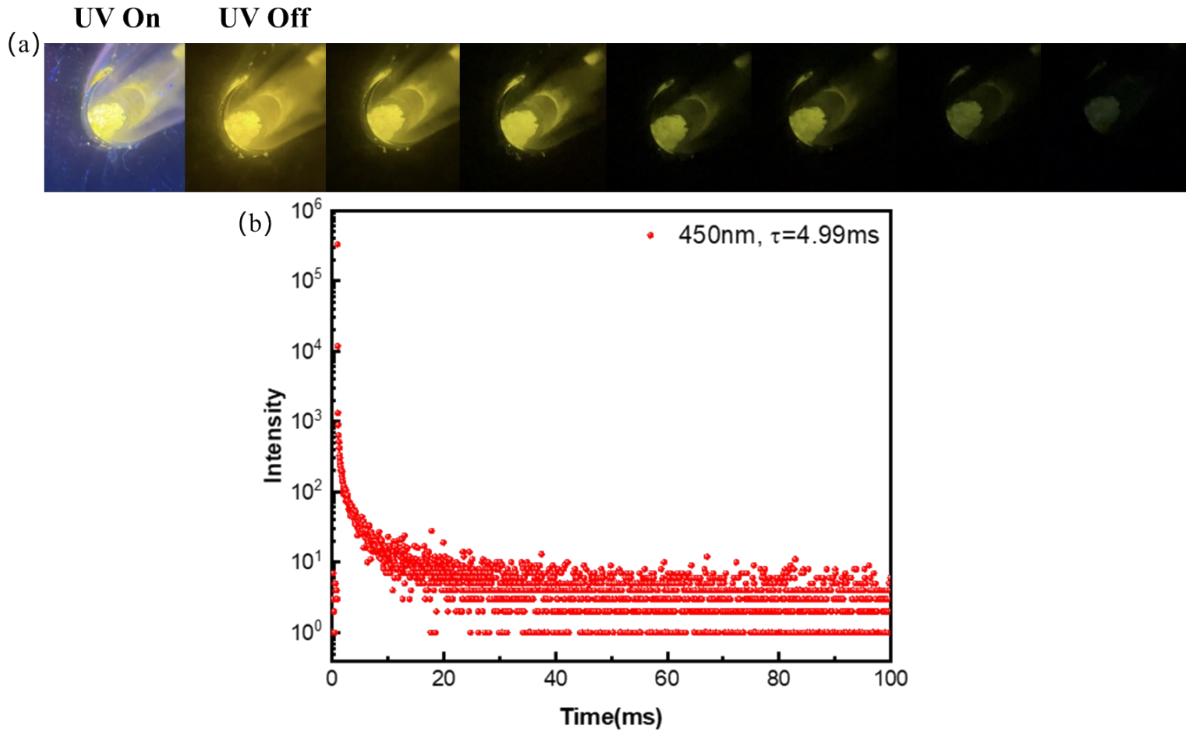

Figure S12. (a) Luminescent images of CN2BCzBr powder at 77 K; (b) decay spectra of CN2BCzBr powder at 77 K. (λ_{ex} = 365 nm)

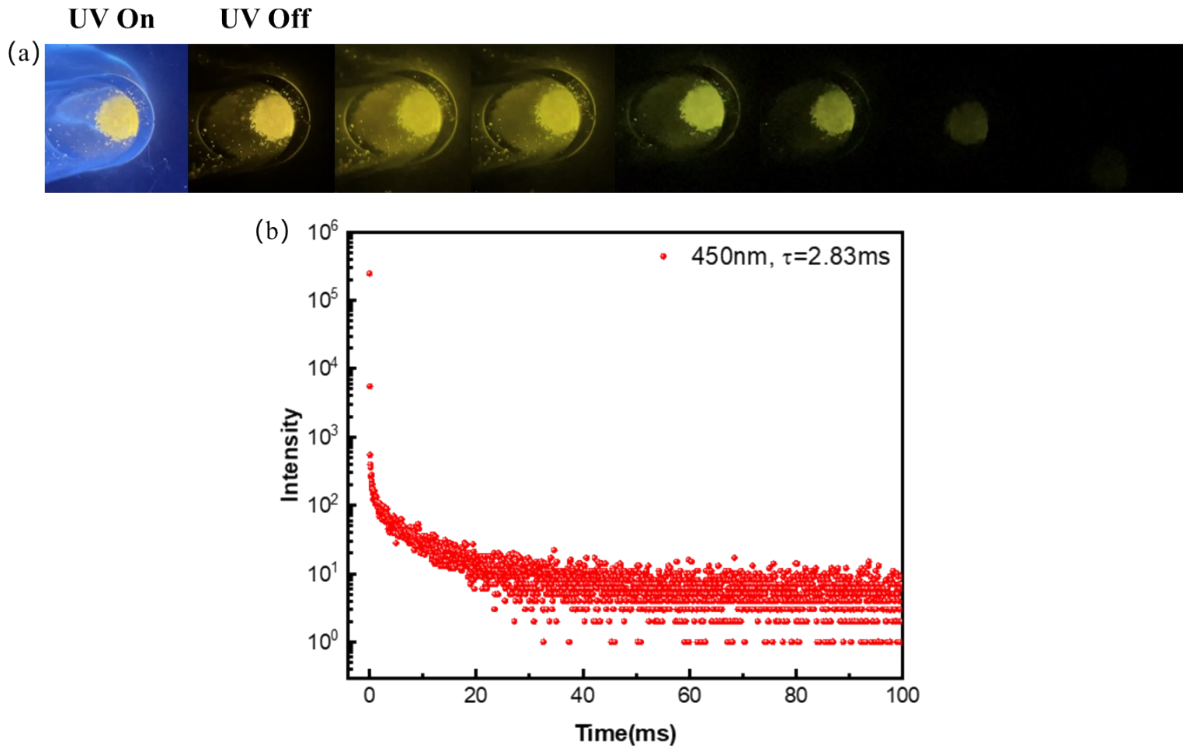

Figure S13. (a) Luminescent images of CNCzBCzBr powder at 77 K; (b) decay spectra of CNCzBCzBr powder at 77 K. (λ_{ex} = 365 nm)

6. Photophysical properties in the PMMA film.

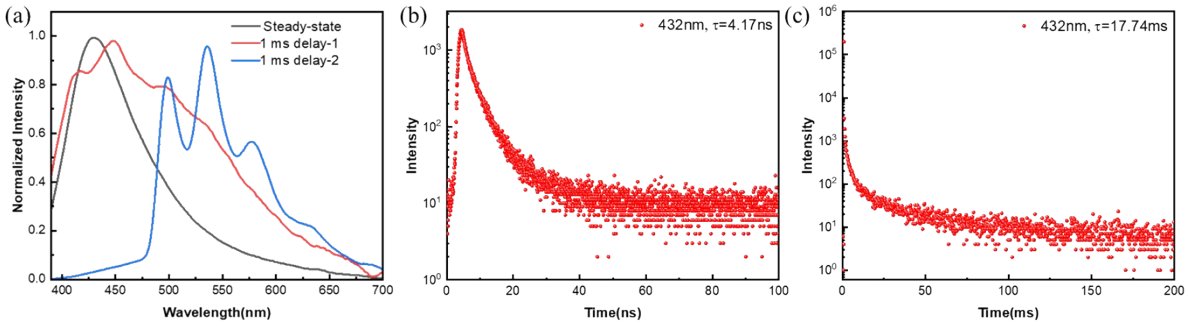

Figure S14. (a) Steady-state and 1 ms-delayed PL spectra of CN2BCzBr@PMMA film (1 wt%); and (b-c) decay spectra at ambient condition. (λ_{ex} = 365 nm)

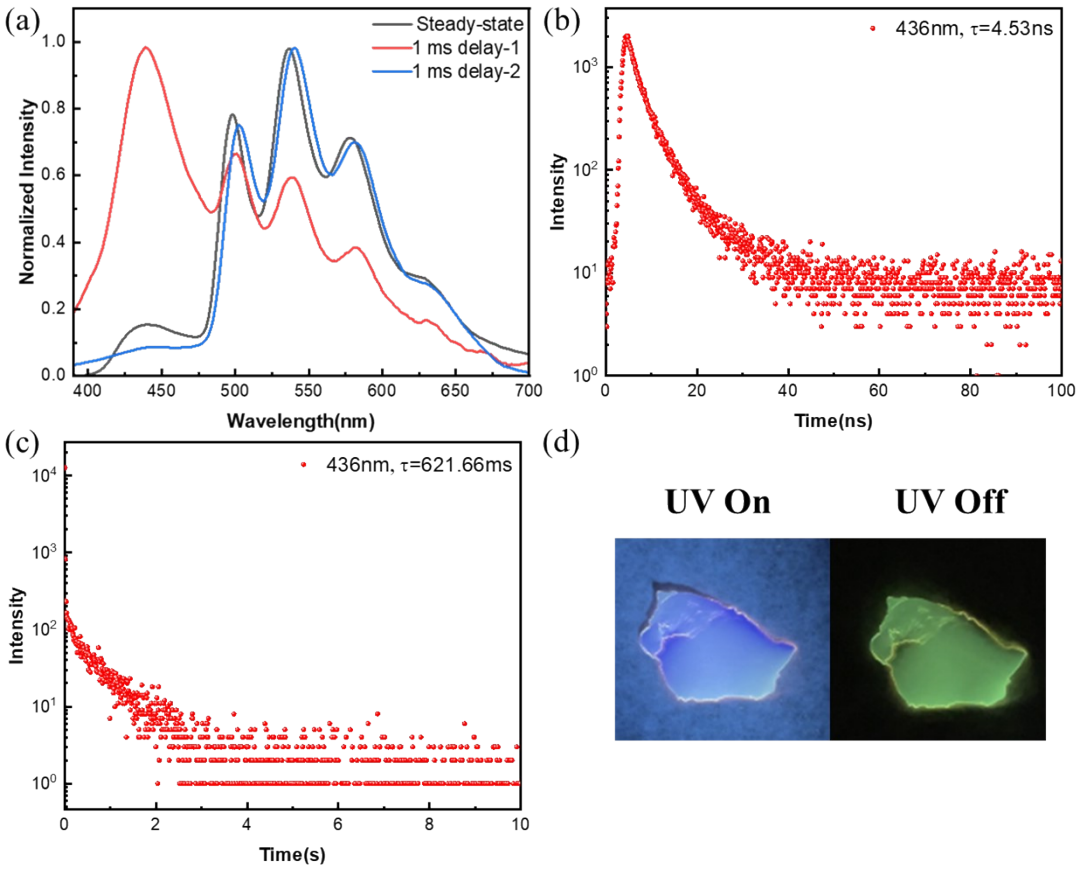

Figure S15. (a) Steady-state and 1 ms-delayed PL spectra of CNCzBCzBr@PMMA film (1 wt%); and (b-c) decay spectra at ambient condition; (d) luminescent images of CNCzBCzBr@PMMA film (1 wt%) after completing the whole photo activation at ambient condition. (λ_{ex} = 365 nm)

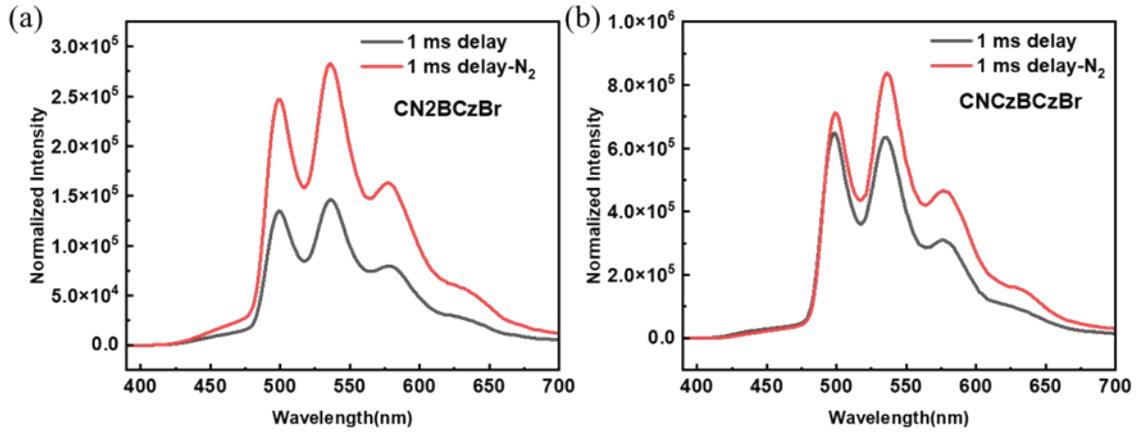

Figure S16. (a) 1 ms-delayed PL spectra at ambient condition and at nitrogen atmosphere of (a) CN2BCzBr@PMMA film (1 wt%) and (b) CNCzBCzBr@PMMA film (1 wt%).

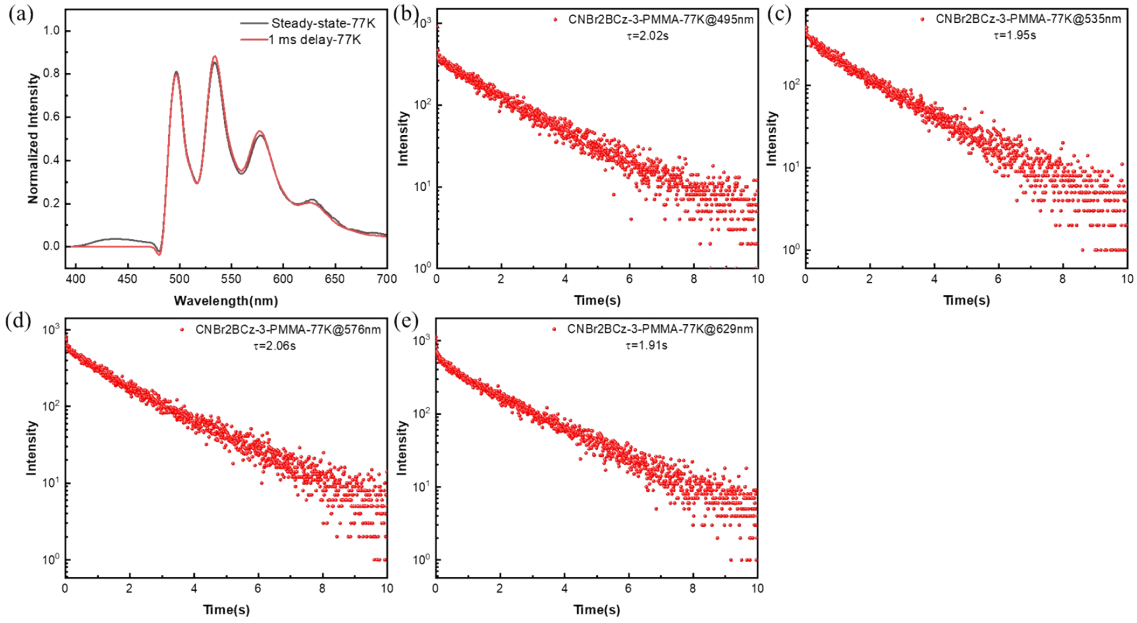

Figure S17. (a) Steady-state and 1 ms-delayed PL spectra of CN2BCzBr@PMMA film (1 wt%); and (b-e) decay spectra of CN2BCzBr@PMMA film (1 wt%) at 77 K. (λ_{ex} = 365 nm)

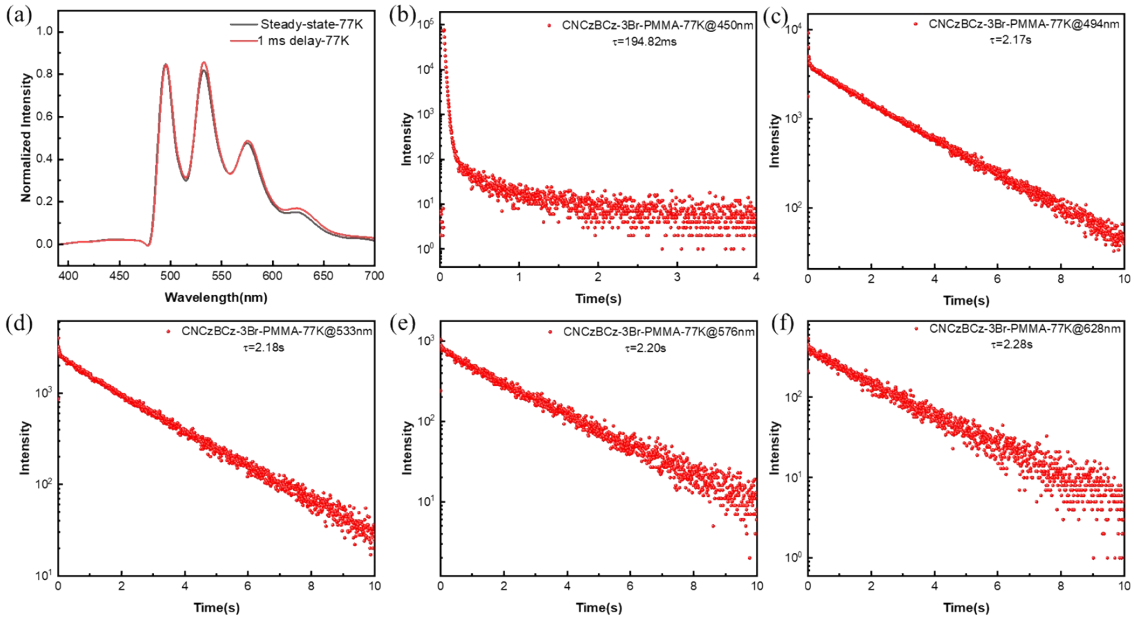

Figure S18. (a) Steady-state and 1 ms-delayed PL spectra of CNCzBCzBr@PMMA film (1 wt%); and (b-f) decay spectra of CNCzBCzBr@PMMA film (1 wt%) at 77 K. (λ_{ex} = 365 nm)

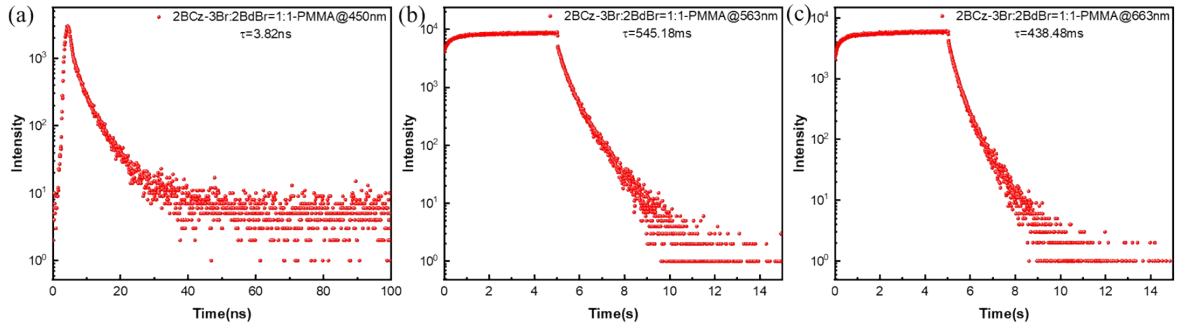

Figure S19. (a) Decay spectra of CN2BCzBr : CN2BdBr@PMMA film (CN2BCzBr : CN2BdBr=1:1) at ambient condition. (λ_{ex} = 365 nm)

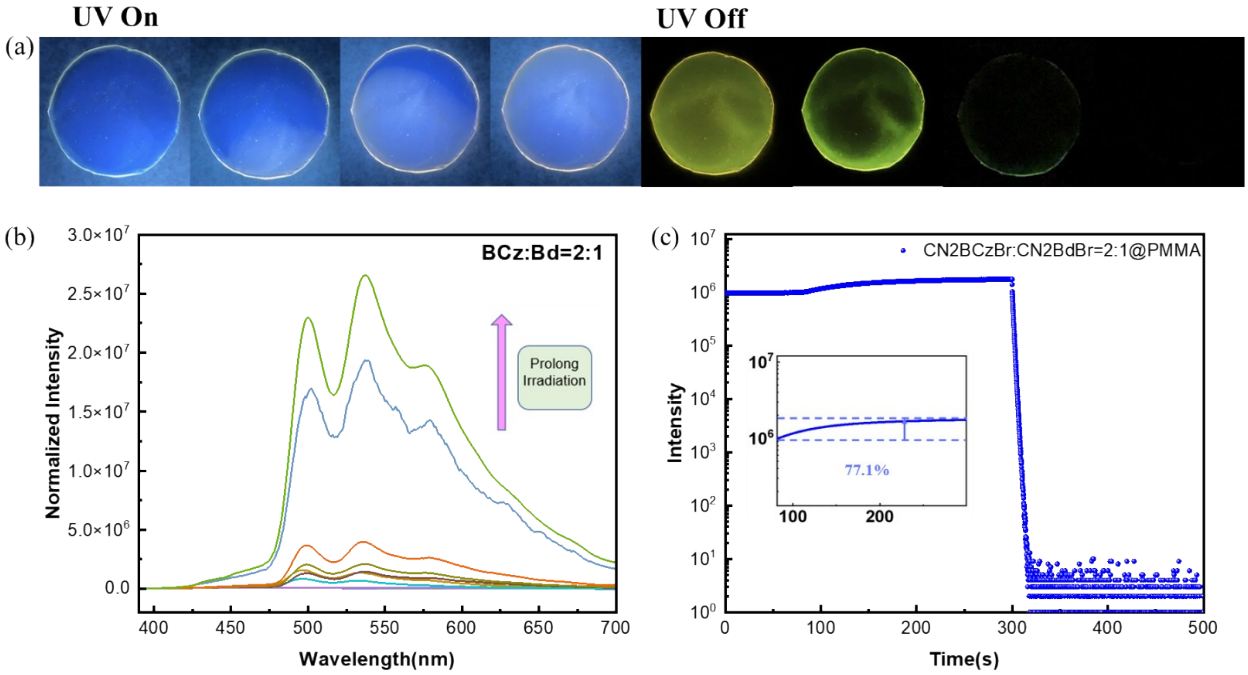

Figure S20. (a) Luminescent images of CN2BCzBr : CN2BdBr@PMMA film (CN2BCzBr : CN2BdBr=2:1) after completing the whole photo activation at ambient condition; (b) the photo-activated phosphorescence enhancement of CN2BCzBr : CN2BdBr@PMMA film (CN2BCzBr : CN2BdBr=2:1) monitored by delayed PL spectra (Δt = 1 ms); (c) the kinetic scanning of the CN2BCzBr : CN2BdBr@PMMA film (CN2BCzBr : CN2BdBr=2:1). (λ_{ex} = 365 nm)

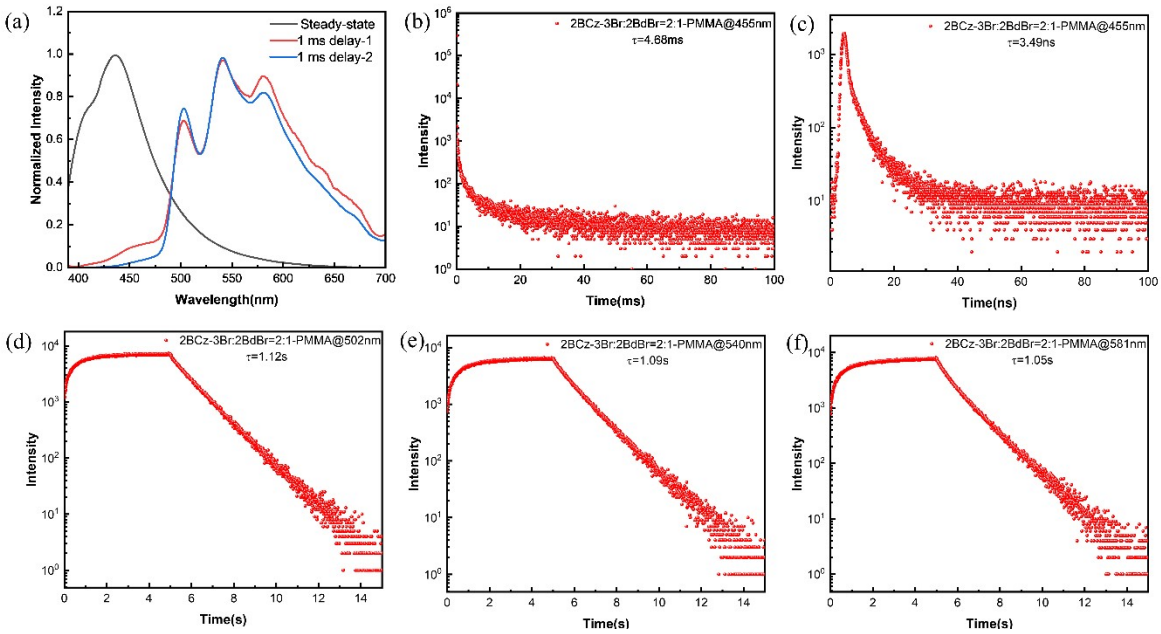

Figure S21. (a) Steady-state and 1 ms-delayed PL spectra of CN2BCzBr : CN2BdBr@PMMA film (CN2BCzBr : CN2BdBr=2:1); and (b-f) decay spectra of CN2BCzBr : CN2BdBr@PMMA film (CN2BCzBr : CN2BdBr=2:1) at ambient condition. (λ_{ex} = 365 nm)

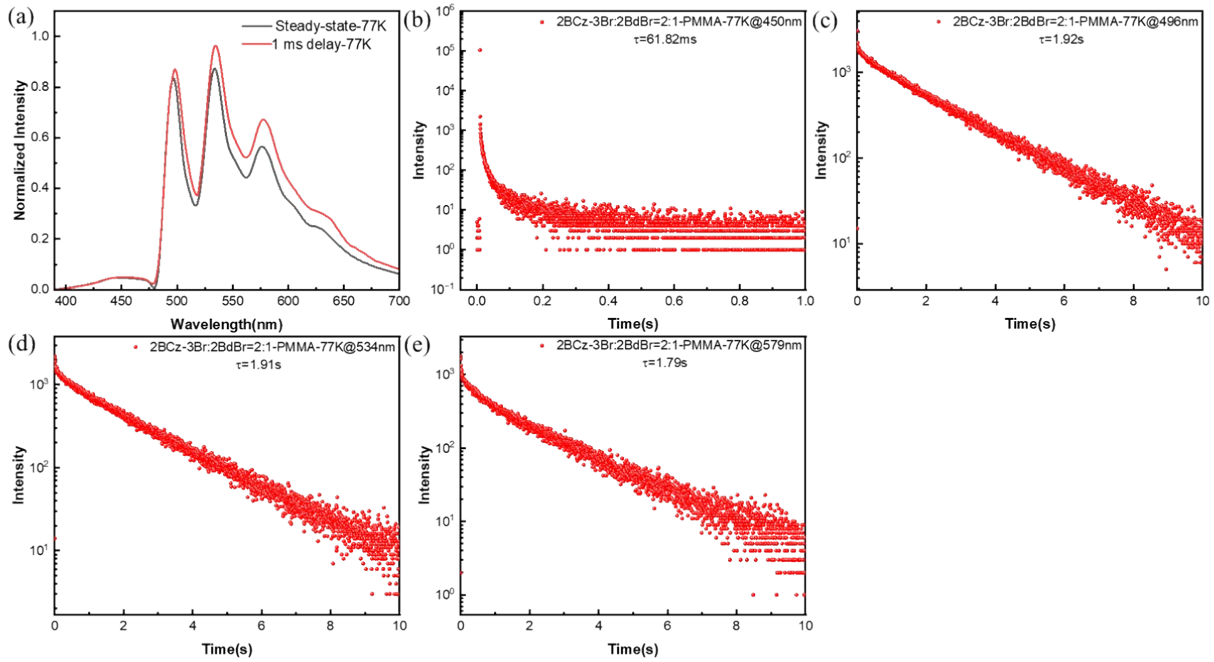

Figure S22. (a) Steady-state and 1 ms-delayed PL spectra of CN2BCzBr : CN2BdBr@PMMA film (CN2BCzBr : CN2BdBr=2:1); and (b-f) decay spectra of CN2BCzBr : CN2BdBr@PMMA film (CN2BCzBr : CN2BdBr=2:1) at 77 K. (λ_{ex} = 365 nm)

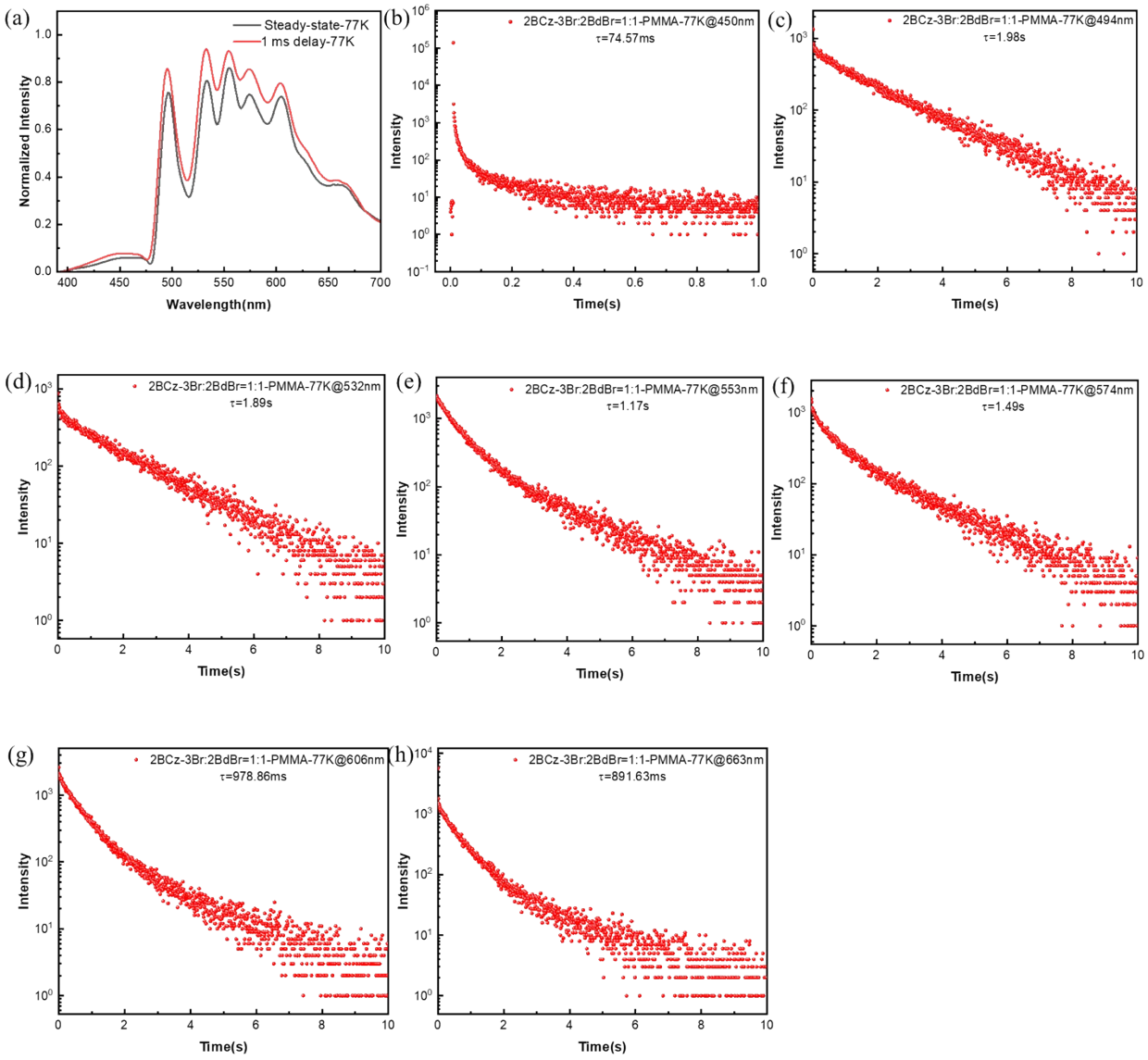

Figure S23. (a) Steady-state and 1 ms-delayed PL spectra of CN2BCzBr : CN2BdBr@PMMA film (CN2BCzBr : CN2BdBr=1:1); and (b-f) decay spectra of CN2BCzBr : CN2BdBr@PMMA film (CN2BCzBr : CN2BdBr=1:1) at 77 K. (λ_{ex} = 365 nm)

7. TD-DFT results

Table S1. The singlet and triplet excited state transition configurations of CN2BCzBr monomer. The matched excited states that contain the same orbital transition components of S1 are shown in bold.

Excited State	Energy (eV)	Transition configuration (%)
T_1	2.5891 eV	**H-3→L(3.30),** H-2→L(2.14), **H-1→L(36.85), H-1→L+1(17.74), H→L(13.08), H→L+1(10.07)**
T_2	2.5911 eV	H-2→L(2.36), **H-2→L+1(3.26), H-1→L(6.58), H-1→L+1(15.98), H→L(20.66), H→L+1(30.63), H→L+2(3.41)**
T_3	3.1955 eV	**H-3→L(24.14),** H-3→L+1(17.27), H-2→L(15.50), **H-2→L+1(11.97), H-1→L(3.90**), H-1→L+1(2.83), H→L(2.71), H→L+1(2.08)
T_4	3.1985 eV	**H-3→L(8.61),** H-3→L+1(14.97), H-3→L+2(4.44), H-2→L(15.15), **H-2→L+1(23.00),** H-2→L+2(6.69), **H→L(2.94), H→L+1(4.86)**
T_5	3.2698 eV	H-9→L+2(11.57), H-8→L+3(10.70), **H-3→L(5.04),** H-3→L+1(2.18), H-3→L+2(19.19), H-2→L+3(5.14), **H-1→L+1(2.40), H-1→L+2(20.65), H→L+3(5.55)**
T_6	3.4720 eV	H-7→L(2.74), H-6→L+1(3.27), H-3→L+1(2.47), H-3→L+3(2.24), H-2→L (6.21), H-2→L+2(5.47), H-1→L+3(6.62), H-1→L+5(5.88), H-1→L+7(2.44), **H→L(2.72), H→L+1(2.80), H→L+2(29.88),** H→L+6(5.55), H→L+8(2.71)
T_7	3.5521 eV	H-7→L+1(7.06), H-6→L (9.87), **H-3→L (3.66), H-2→L+1(3.44),** H-1→L+3(5.34), H-1→L+5(4.56), H-1→L+6(7.43), H-1→L+8(8.13), **H→L+2(2.92),** H→L+5(8.10), H→L+6(2.15), H→L+7(7.17)
T_8	3.5872 eV	H-7→L(2.86), H-6→L+1(2.43), H-2→L+3(2.07), H-1→L (3.95), H-1→L+1(2.38), H-1→L+2(9.77), H-1→L+3(2.59), H-1→L+7(4.38), **H→L+1(5.79), H→L+2(19.58),** H→L+3(14.12), H→L+6(3.61), H→L+8(4.99)

S_1	**3.6179 eV**	**H-3→L(2.63), H-2→L+1(3.56), H-1→L(7.70), H-1→L+1(8.35), H-1→L+2(11.35), H→L(3.80), H→L+1(34.69), H→L+2(20.94)**
S_2	3.6264 eV	H-3→L+1(4.76), H-2→L(6.98), **H-1→L(2.44), H-1→L+1(28.91), H→L(45.86), H→L+1(2.52)**
T_9	3.6508 eV	H-8→L+3(4.06), H-2→L+3(14.30), **H-1→L(2.22), H-1→L+2(16.93),** H-1→L+5(2.75), **H→L(5.62), H→L+2(13.62),** H→L+3(15.38), H→L+6(3.51), H→L+8(2.11)
S_3	3.6509 eV	**H-3→L(3.30), H-2→L+1(2.11),** H-2→L+2(2.36), **H-1→L (17.58), H-1→L+2(3.56), H→L+1(3.85), H→L+2(59.85)**
T_{10}	3.6775 eV	H-3→L+2(9.30), H-3→L+3(8.29), **H-1→L+1(9.23), H-1→L+2(16.10),** H-1→L+3(14.36), H-1→L+5(2.29), H-1→L+6(2.49), **H→L(8.34),** H→L+3(12.61), H→L+5(2.78)
S_4	3.6840 eV	**H-1→L(31.25), H-1→L+1(7.11), H-1→L+2(47.14), H→L+1(2.37), H→L+2(3.71)**
T_{11}	3.7002 eV	H-3→L+2(15.72), H-3→L+3(8.74), **H-1→L(3.91), H-1→L+2(2.91),** H-1→L+3(32.90), **H→L+2(8.32),** H→L+3(10.61)
S_5	3.7432 eV	**H-1→L(8.05), H-1→L+1(7.03),** H-1→L+3(14.40), **H→L(14.41), H→L+1(21.92),** H→L+3(27.12)
T_{12}	3.7531 eV	H-3→L+3(6.23), H-2→L(2.10), **H-2→L+1(5.68),** H-2→L+2(48.68), H-1→L+3(3.90), H-1→L+5(6.37), **H→L+2(3.92),** H→L+6(7.24)
S_6	3.7714 eV	**H-3→L(2.03),** H-2→L(3.72), **H-1→L+2(7.46),** H-1→L+3(49.63), H→L+3(27.45)
T_{13}	3.8200 eV	H-3→L+3(2.18), H-2→L+3(2.74), **H-1→L(13.67), H-1→L+1(9.69),** H-1→L+3(6.14), **H→L(30.44), H→L+1(24.69),** H→L+3(4.94)
T_{14}	3.8257 eV	**H-1→L(19.48), H-1→L+1(29.30), H-1→L+2(16.64), H→L(9.18), H→L+1(12.56), H→L+2(6.39)**

S_7	3.8299 eV	H-2→L(3.25), **H-2→L+1(2.82),** H-2→L+2(4.21), **H-1→L(11.46), H-1→L+1(23.09), H-1→L+2(15.85),** H-1→L+3(3.85), **H→L(9.63), H→L+1(14.95), H→L+2(5.39),** H→L+3(2.25)
S8	3.8400 eV	H-3→L+1(5.77), H-2→L(10.92), **H-2→L+1(3.48), H-1→L(6.27), H-1→L+1(19.11), H-1→L+2(2.44),** H-1→L+3(15.68), **H→L(7.17), H→L+1(8.18),** H→L+3(13.20)
S9	3.8485 eV	H-3→L+1(2.55), H-2→L(17.98), **H-2→L+1(8.33),** H-2→L+2(14.36), **H-1→L(6.78), H-1→L+1(2.52), H-1→L+2(8.75),** H-1→L+3(3.73), **H→L(11.94), H→L+1(2.65),** H→L+3(15.25)
T15	3.8721 eV	H-7→L+1(2.47), H-5→L+1(2.66), H-4→L(2.52), **H-3→L(2.52),** H-3→L+3(2.67), H-3→L+6(3.65), H-3→L+8(4.52), H-2→L+5(3.16), H-2→L+7(4.25), **H-1→L(2.29), H-1→L+2(2.45),** H-1→L+5(2.32), H-1→L+6(7.15), H-1→L+8(4.16), **H→L+1(2.43),** H→L+5(6.94), H→L+6(5.65), H→L+7(5.45)
S10	3.8751 eV	**H-3→L(37.93),** H-3→L+2(2.81), H-2→L(4.14), **H-2→L+1(23.09), H-1→L(4.23),** H-1→L+3(2.08), H-1→L+5(3.55), H-1→L+6(2.23), **H→L+1(5.01),** H→L+3(2.67), H→L+5(3.41)
T16	3.8783 eV	H-8→L+3(2.70), H-5→L(2.45), H-3→L+2(2.82), H-3→L+5(3.88), H-3→L+7(2.78), H-2→L(6.83), H-2→L+2(10.52), H-2→L+3(7.97), H-2→L+6(2.05), **H-1→L+1(3.68),** H-1→L+5(7.44), H-1→L+7(4.84), **H→L+2(2.81),** H→L+3(3.01), H→L+6(6.91), H→L+8(4.59)
S11	3.9045 eV	**H-3→L(4.96),** H-3→L+1(31.25), H-3→L+2(15.11), H-2→L+2(31.48), **H→L+2(4.01),** H→L+3(2.49), H→L+6(2.65)
T17	3.9112 eV	H-8→L+3(2.36), H-4→L+1(2.92), **H-3→L(3.56),** H-3→L+2(8.94), H-3→L+7(3.19), **H-2→L+1(2.59),** H-2→L+3(18.50), H-2→L+8(3.98), **H-1→L+2(3.31),**

		H→L+3(22.69)

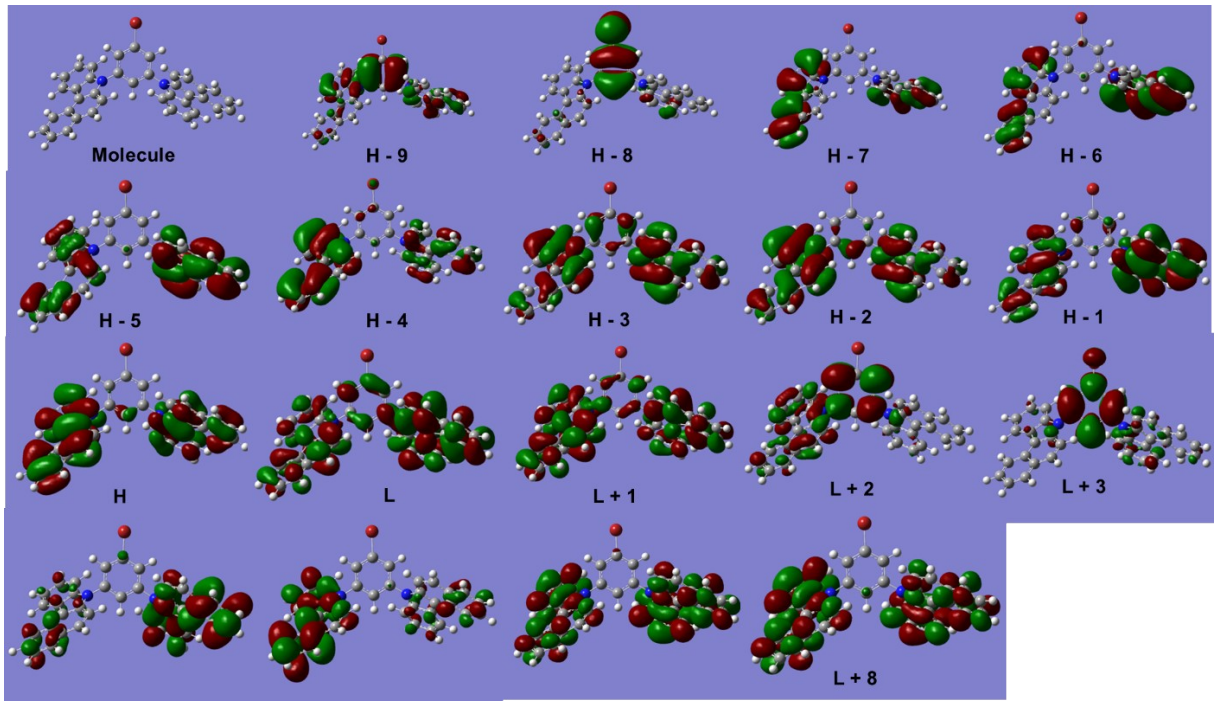

Figure S24. Plots of CN2BCzBr monomer visualized orbitals.

Table S2. The singlet and triplet excited state transition configurations of CNCzBCzBr monomer. The matched excited states that contain the same orbital transition components of S1 are shown in bold.

Excited State	Energy (eV)	Transition configuration (%)
T_1	2.5922eV	**H-2→L(8.44), H→L(75.25),** H→L+1(3.17)
T_2	3.1600eV	H-6→L+3(2.97), H-3→L+3(75.52), H-1→L+6(5.43), H-1→L+7(5.71)
T_3	3.1954eV	H-4→L(2.78), **H-2→L(64.02),** H-2→L+1(8.30), **H→L(10.48),** H→L+1(2.18)
T_4	3.2511eV	H-8→L+1(8.59), H-7→L+2(7.60), H-6→L+2(2.44), **H-2→L(2.91),** H-2→L+1(8.83), H-1→L(5.22), H-1→L+1(27.67), H-1→L+2(10.24), H-1→L+3(5.88), H→L+1(6.34), H→L+2(2.17)
T_5	3.3466eV	H-8→L+1(2.56), H-7→L+2(2.23), H-2→L+1(2.86), H-1→L+3(75.40), H→L+1(4.82)
T_6	3.5016eV	H-5→L(8.45), **H-2→L(7.36),** H-2→L+9(2.02),

		H-1→L(3.98), H-1→L+1(9.42), H-1→L+2(3.27), H-1→L+3(6.47), H→L+1(22.12), H→L+5(13.69), H→L+6(3.33), H→L+7(3.32)
T_7	3.6047eV	H-5→L(8.64), H-4→L(3.52), **H-2→L(2.04),** H-1→L(2.19), H-1→L+1(10.01), H-1→L+3(2.77), H→L+1(14.83), H→L+2(20.21), H→L+5(8.20), H→L+6(5.76), H→L+7(5.04)
S_1	**3.6233eV**	**H-2→L(11.93), H-2→L+5(2.76), H→L(77.22)**
T_8	3.6681eV	H-7→L+2(4.40), H-2→L+1(2.52), H-2→L+2(6.05), H-1→L+1(11.69), H-1→L+2(30.82), H→L+1(10.90), H→L+2(19.08), H→L+5(2.72)
S_2	3.6727 eV	H-2→L+1(2.96), H-1→L+1(5.04), H→L+1(85.80)
T_9	3.7130 eV	H-8→L+2(2.33), H-2→L+2(13.54), H-1→L+1(6.20), H-1→L+2(38.01), H→L+1(15.43), H→L+2(16.54)
T_{10}	3.7406 eV	H-2→L+1(33.61), H-2→L+2(2.90), H-1→L(2.19), H-1→L+1(8.87), H→L+1(11.25), H→L+2(12.82), H→L+5(12.37)
S_3	3.7742 eV	H-1→L(19.61), H-1→L+1(55.70), **H→L(5.53),** H→L+1(2.31), H→L+2(13.12)
S_4	3.7928 eV	**H-2→L(7.64),** H-2→L+2(3.18), H-1→L(3.47), H-1→L+1(5.69), H→L+1(2.17), H→L+2(74.06)
S_5	3.8674 eV	**H-2→L(7.87),** H-2→L+1(5.49), H-1→L(3.19), H-1→L+2(78.87)
S_6	3.8725 eV	**H-2→L(53.43),** H-2→L+1(2.02), H-1→L+1(6.76), H-1→L+2(9.96), **H→L(8.63),** H→L+1(3.61), H→L+2(4.58), H→L+5(6.85)
T_{11}	3.8786 eV	H-5→L(4.55), H-5→L+1(2.07), H-5→L+5(2.87), H-4→L(4.94), **H-2→L(3.59),** H-2→L+1(9.82), H-2→L+2(2.67), **H-2→L+5(8.98),** H-2→L+6(4.05), H-2→L+7(4.01), **H→L(4.33),** H→L+5(18.73), H→L+6(5.74), H→L+7(5.68)
T_{12}	3.9258 eV	H-7→L(3.75), H-4→L+1(7.53), H-2→L+1(14.07), H-2→L+2(32.44), **H-2→L(4.29),** H-2→L+1(4.19),

		H→L+2(3.27), H→L+5(15.58)

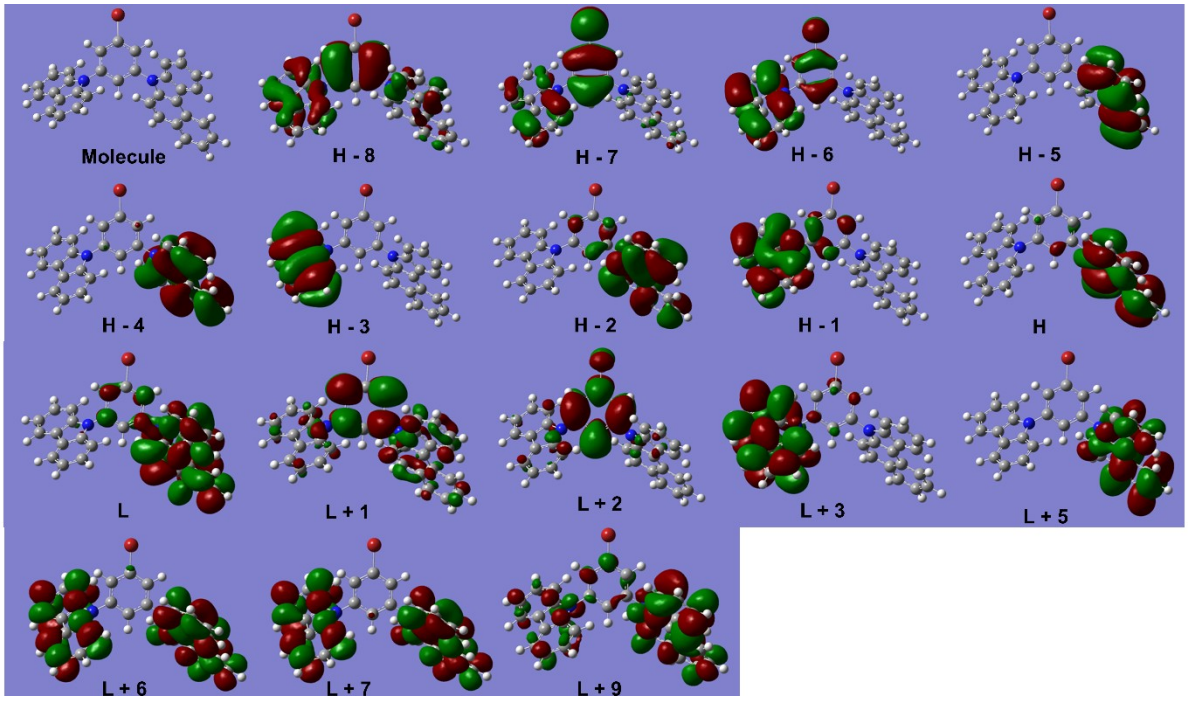

Figure S25. Plots of CNCzBCzBr monomer visualized orbitals.

Table S3. Spin-orbit coupling (SOC) values between S_n and T_n of CN2BCzBr and CNCzBCzBr monomer.

<S_n|Hso|T_n>	**CN2BCzBr (cm^{-1})**	**CNCzBCzBr (cm^{-1})**
S_0/T_1	16.05333	10.17893
S_0/T_2	11.00925	10.09428
S_0/T_3	54.48844	34.11163
S_0/T_4	33.72405	67.85294
S_0/T_5	72.62601	28.15705
S_0/T_6	162.56822	126.38018

S_0/T_7	94.35802	163.22569
S_0/T_8	132.46187	274.50186
S_0/T_9	203.25560	366.66217
S_0/T_{10}	211.09846	60.89635
S_0/T_{11}	242.53845	96.70079
S_0/T_{12}	104.20704	104.75276
S_0/T_{13}	224.72096	-
S_0/T_{14}	83.83977	-
S_0/T_{15}	86.94891	-
S_0/T_{16}	60.57689	-
S_0/T_{17}	48.48906	-
S1/T1	5.60881	29.71356
S1/T2	15.55844	0.71253
S1/T3	5.65310	23.58924
S1/T4	14.75922	111.50197
S1/T5	104.24928	51.34317
S1/T6	44.01730	18.03251
S1/T7	36.52493	76.98869
S1/T8	52.89971	105.26272

S1/T9	11.70254	66.78940
S1/T10	64.39703	42.40035
S1/T11	81.62939	13.31195
S1/T12	47.60446	15.58617
S1/T13	57.97989	-
S1/T14	32.86419	-
S1/T15	2.49576	-
S1/T16	9.97872	-
S1/T17	21.56207	-

Table S4. The excited state and oscillator strength of CN2BCzBr and CNCzBCzBr monomer radical.

Excited State	**Energy (eV)**	**Wavelength (nm)**	**oscillator strength (f)**
CN2BCzBr			
ES7	**1.5491**	**800.38**	**0.0679**
ES9	2.1983	564.00	0.0472
CNCzBCzBr			
ES7	**1.5998**	**775.01**	**0.0695**
ES8	2.0419	607.21	0.0393
ES9	2.1967	564.41	0.0393

Table S5. Total energy of CN2BCzBr and CNCzBCzBr monomer and their radical cations.

	CN2BCzBr	CNCzBCzBr
Monomer (E_M,HF)	-4145.98679895	-3992.31007742
Radical ($E_{M^{\cdot+}}$,HF)	-4145.73865089	-3992.05754292
ΔE ($E_{M^{\cdot+}} - E_M$, kJ/mol)	651.51	663.03

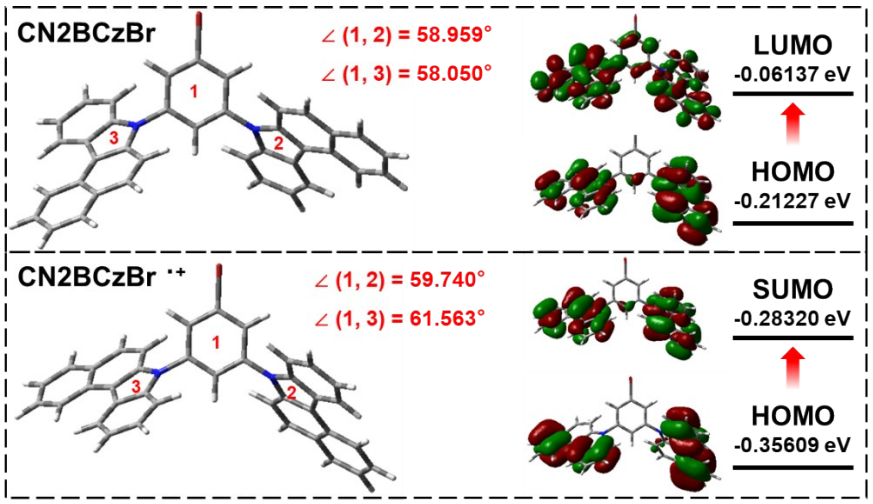

Figure S26. Plots of CN2BCzBr monomer and radical visualized orbitals.

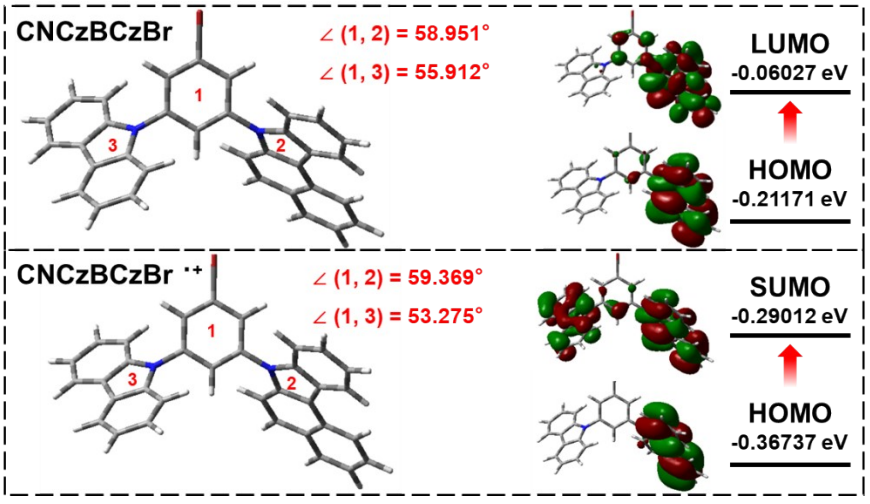

Figure S27. Plots of CNCzBCzBr monomer and radical visualized orbitals.

References

(1) Li, J.-A.; Zhou, J.; Mao, Z.; Xie, Z.; Yang, Z.; Xu, B.; Liu, C.; Chen, X.; Ren, D.; Pan, H.; Shi, G.; Zhang, Y.; Chi, Z. Transient and Persistent Room-Temperature Mechanoluminescence from a White-Light-Emitting AIEgen with Tricolor Emission Switching Triggered by Light. *Angew. Chem. Int. Ed.* **2018,** *57*, 6449-6453.

(2) An, Z.; Zheng, C.; Tao, Y.; Chen, R.; Shi, H.; Chen, T.; Wang, Z.; Li, H.; Deng, R.; Liu, X.; Huang, W. Stabilizing triplet excited states for ultralong organic phosphorescence. *Nat. Mater.* **2015,** *14*, 685-690.

(3) Liu, Y.; Ma, Z.; Cheng, X.; Qian, C.; Liu, J.; Zhang, X.; Chen, M.; Jia, X.; Ma, Z. Regulating force-resistance and acid-responsiveness of pure organics with persistent phosphorescence via simple isomerization. *J. Mater. Chem. C* **2021,** *9*, 5227-5233.

(4) Qian, C.; Ma, Z.; Yang, B.; Li, X.; Sun, J.; Li, Z.; Jiang, H.; Chen, M.; Jia, X.; Ma, Z. Carbazole&benzoindole-based purely organic phosphors: a comprehensive phosphorescence mechanism, tunable lifetime and an advanced encryption system. *J. Mater. Chem. C* **2021,** *9*, 14294-14302.